Electronic Supplementary Material (ESI) for Dalton Transactions.
This journal is © The Royal Society of Chemistry 2014

Heteroligand hydroxocopper(II)/pyridazine clusters embedded into 3D framework lattices

Anna S. Degtyarenko,[a] Marcel Handke,[b] Karl W. Krämer,[c] Shi-Xia Liu,*[c] Silvio Decurtins,[c] Eduard B. Rusanov,[d] Laurence K. Thompson,[e] Harald Krautscheid[b] and Konstantin V. Domasevitch*[a]

[a] Inorganic Chemistry Dpt, Taras Shevchenko National University of Kyiv, Volodimirska Str. 64/13, Kyiv 01601, Ukraine. E-mail: dk@univ.kiev.ua

[b] Institut für Anorganische Chemie, Universität Leipzig, Johannisallee 29, D-04103 Leipzig, Deutschland

[c] Departement für Chemie und Biochemie, Universität Bern, Freiestrasse 3, CH-3012 Bern, Switzerland

[d] Institute of Organic Chemistry, Murmanskaya Str.4, Kyiv 253660, Ukraine

[e] Department of Chemistry, Memorial University of Newfoundland, St. John's, Canada

SUPPORTING INFORMATION

CONTENTS

1. ORGANIC SYNTHESES

1.1. 1,3-Dibromoadamantane

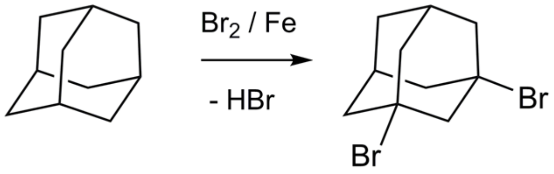

Bromination is a key first step for the most strategies for functionalization of adamantane. All four stages of bromination at the bridge-head positions proceed smoothly yet selectively, depending on the reaction conditions (See: Senchyk, G. A., Lysenko, A. B., Boldog, I., Rusanov, E. B., Chernega, A. N., Krautscheid, H., Domasevitch K. V. *Dalton Trans*., **2012**, *41*, 8675). For selective dibromination, the best procedure implies reaction of adamantane with net bromine at ambient conditions under the presence of Fe powder. This gives the desired product in actually quantitative yield, with no mono- and tribrominated co-products. The reaction may be readily scaled and it proceeds equally well for the 0.5 g – 500 g batch scales of starting adamantane.

10.0 g of Fe powder was added at once with stirring to 400 mL bromine, pre-cooled in an ice-bath. The stirring was continued for 30 min and then 137.1 g of solid adamantane was added in 15-20 g portions over 30 min, with efficient stirring. HBr gas, extensively evolved during the addition of adamantane, was trapped by passing over ice water. The mixture was stirred for 1 h at r.t. and poured onto 2 kg of finely crushed ice mixed with solid Na_2SO_3 (0.8 kg). Solid brown-black precipitate was carefully triturated and powdered under the solution (with external cooling, when necessary) until disappearance of the brown bromine coloration. The product was filtered and repeatedly washed with 1:10 HCl solution and with water and dried in air. Recrystallization from 2-propanol with charcoal gives pure 1,3-dibromoadamantane as colorless crystals with m.p. = 111-112^{o}C. The yield was 247.3 g (83%). Evaporation of the 2-propanol filtrates and recrystallization of the combined residues provides additional portion of the pure product and the total yield was 286.0 g (96%).

1.2. 1,3-*bis*(2,2-dibromoethyl)adamantane

Vinyl bromide (bp = 16-17^{o}C) was prepared in 85% yield reacting 1,2-dibromoethane and ethanolic KOH solution (following the procedure for 10 g batch scale synthesis of vinyl-*d* bromide, See J.P. Schaefer, M.J. Dagan, and D.S. Weinberg, *J. Am. Chem. Soc.*, **1967**, *89*, 6938-6944) and the product was distilled off using the low-temperature condenser. Prior the synthesis, vinyl bromide was freshly purified by additional destillation.

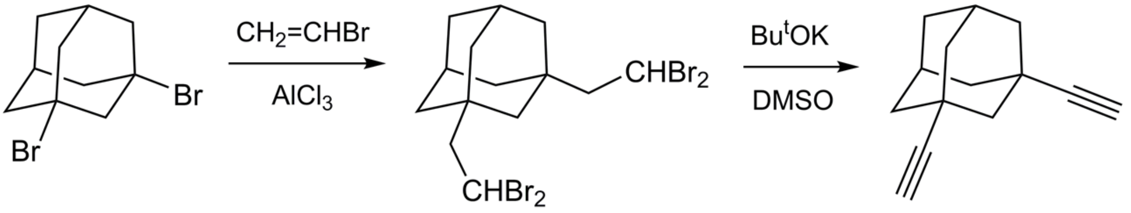

In the next step (for general procedure, See T.G. Archibald, A.A. Malik, and K. Baum, *Macromolecules* **1991**, *24*, 5261), 71.6 g (0.244 mol) of 1,3-dibromoadamantane and 430 ml of dry dichloromethane were placed into the flask equipped with efficient magnetic stirring bar and low-temperature termometer. The solution was cooled to -20°C in an acetone/ liquid nitrogen bath. 65.5 ml of vinyl bromide was added and then 10.47 g of anhydrous $AlCl_3$ (0.080 mol) was added in small portions over the period of 2 h, under efficient stirring. The mixture was stirred for additional 30 min at -15-20° and then poured into 220 ml of 1:3 aqueous HCl solution. The organic layer was separated and the aqueous layer was extracted with CH_2Cl_2 (3 × 150 ml). The combined dichloromethane extracts were washed with 150 ml water, dried over Na_2SO_4 overnight and evaporated under reduced pressure giving dark-brown oil. This product was used in the next step without additional purification.

1.3. 1,3-diethynyladamantane

1,3-bis(2,2-dibromoethyl)adamantane (123.7 g, 0.244 mol) was dissolved in 500 ml of dry DMSO, the solution was heated to 40-45°C and 130.3 g of solid potassium tert-butylate (1.162 mol) was added in 7-10 g portions over 1 h, with stirring. Then the mixture was stirred for 20 h at r.t. and poured onto 0.5 kg of crushed ice acidified with 5 ml conc. HCl. The organic layer was separated and the aqueous layer was repeatedly extracted with dichloromethane (3 × 150 ml). The combined organic layer and dichloromethane extracts were washed with brine and with cold water, dried over Na_2SO_4 and evaporated. The resulting oily product was dried under reduced pressure (70°C, 0.5 mm Hg) and recrystallized from methanol giving 18.0 g (40%) of colorless crystalline product.

1.4. 1,3-*bis*(pyridazin-4-yl)adamantane

The final product was prepared by inverse electron demand Diels-Alder cycloaddition of 1,3-diethynyladamantane and 1,2,4,5-tetrazine, as extreme electron deficient and reactive azadiene component. The efficient large-scale preparation and purification of 1,2,4,5-tetrazine was descibed previously, in supplementary data for publication of A. S. Degtyarenko, P. V.

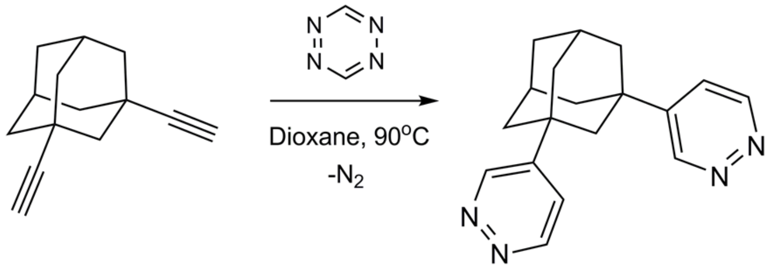

Solntsev, H. Krautscheid, E. B. Rusanov, A. N. Chernega and K. V. Domasevitch, *New J. Chem.*, **2008**, *32*, 1910. For other inverse electron demand cycloadditions of 1,2,4,5-terazine, See J. Sauer, D. K. Heldmann, J. Hetzenegger, J. Krauthan, H. Sichert, J. Schuster, *Eur. J. Org. Chem.* **1998**, 2885.

A solution of 1.24 g (15.1 mmol) 1,2,4,5-tetrazine and 1.26 g (6.8 mmol) 1,3-diethynyladamantane in 40 ml of dry 1,4-dioxane was stirred at 90 ºC over a period of 25 h. The reaction proceeded smoothly and the evolution of dinitrogen gas ceased after first 15-16 h. The precipitate was filtered off, washed with 1,4-dioxane and diethyl ether and dried in air. It was dissolved in boiling methanol, the solution was decolorized by 15 min reflux with charcoal, then it was filtered and evaporated yielding 1.41 g (71%) of colorless crystalline product.

^{1}H NMR (400 MHz, dmso-d$_6$): δ 9.38–9.28 (m, 2H), 9.06 (d, J = 5.4 Hz, 2H), 7.58 (dd, J = 5.5, 2.6 Hz, 2H), 2.42–2.32 (m, 2H), 2.10 (s, 2H), 1.98 (t, J = 3.7 Hz, 8H), 1.82 (d, J = 3.5 Hz, 2H). Anal. Calcd for $C_{18}H_{20}N_4$: C, 73.94; H, 6.90; N, 19.17. Found: C, 74.06; H, 6.88; N, 19.04.

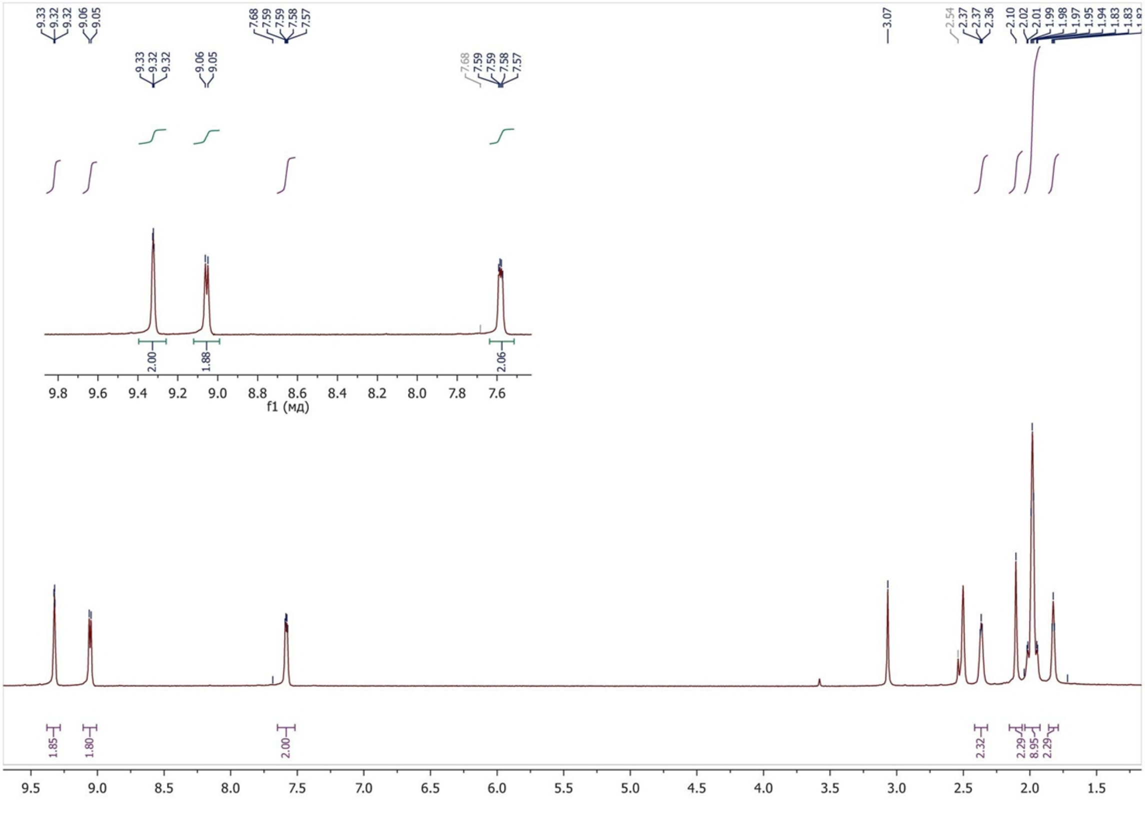

Figure S1. ^{1}H NMR spectrum of 1,3-*bis*(pyridazin-4-yl)adamantane (400 MHz, dmso-d$_6$).

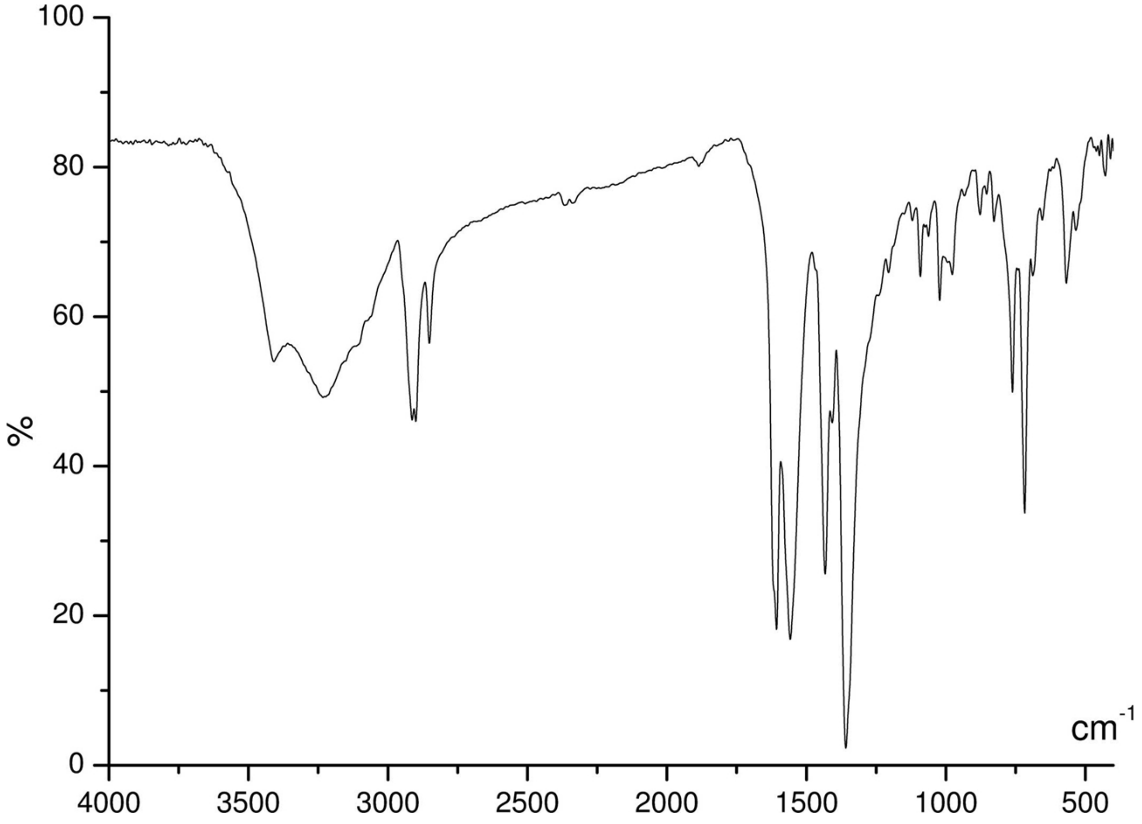

Figure S2. IR spectrum (KBr disk) of *[Cu_2(μ-OH){TMA}(L)(H_2O)]* (**1**).

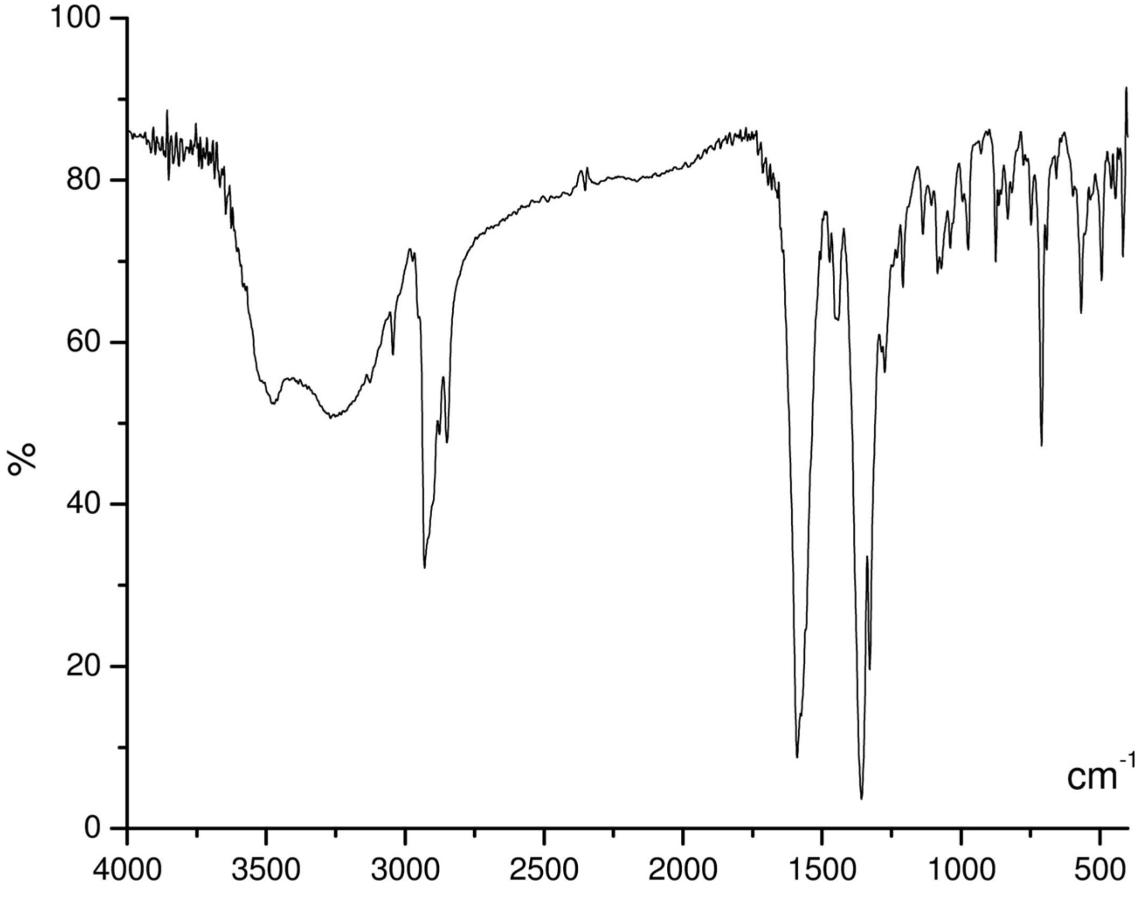

Figure S3. IR spectrum (KBr disk) of *[Cu_4(μ_3-OH)$_2${ATC}$_2$(L)$_2$(H_2O)$_2$]·H_2O* (**2**)

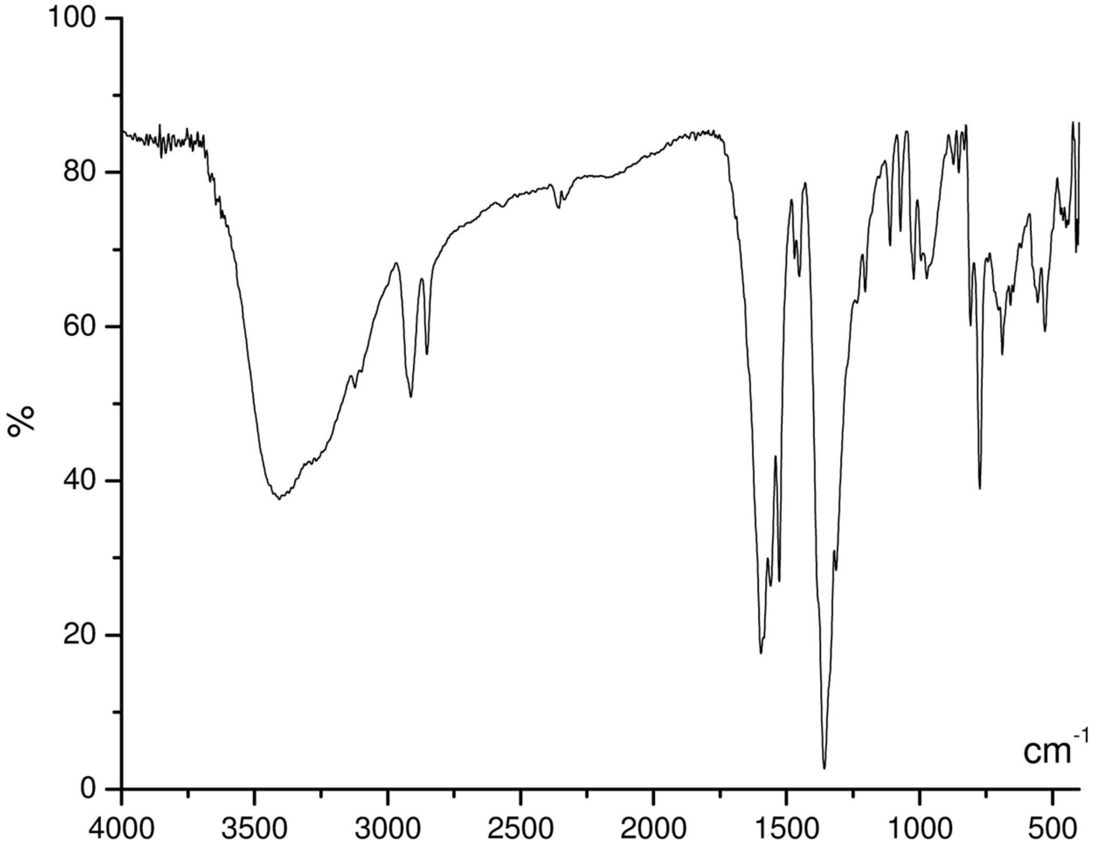

Figure S4. IR spectrum (KBr disk) of $[Cu_4(\mu_3\text{-}OH)_2\{TDC\}_3(L)_2(H_2O)_2]\cdot 7H_2O$ (**3**).

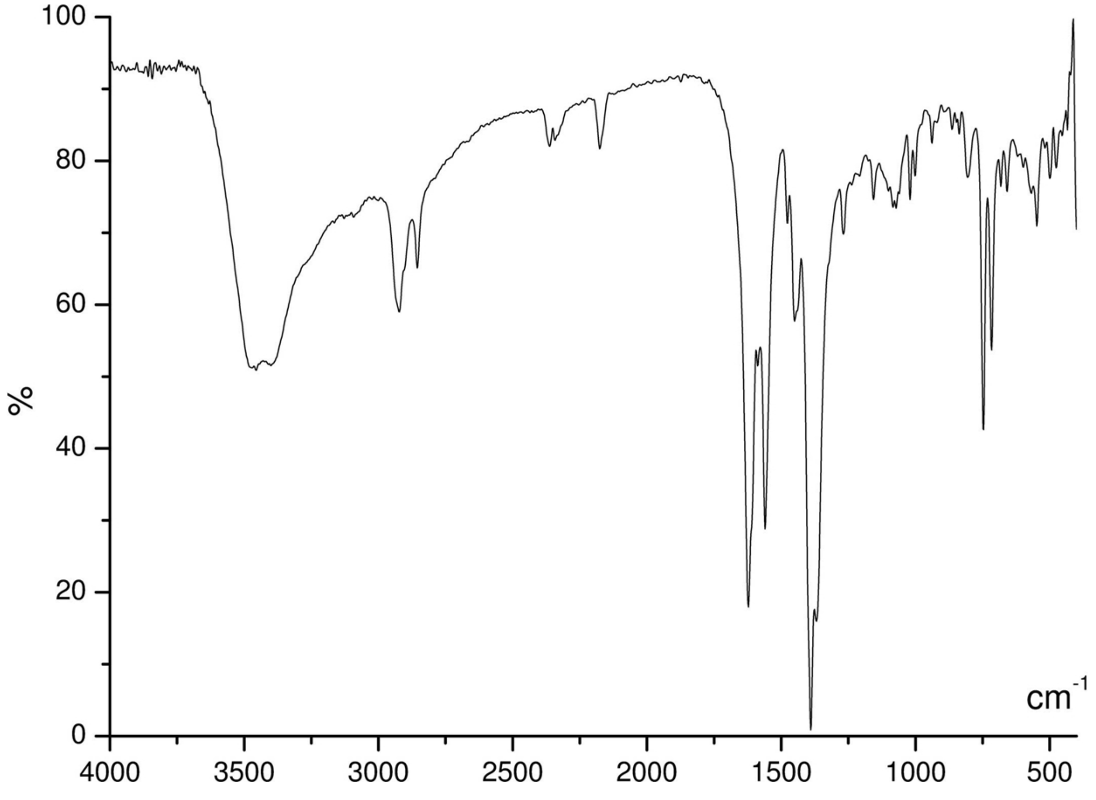

Figure S5. IR spectrum (KBr disk) of $[Cu_5(\mu\text{-}OH)_2\{BDC\}_4(L)_2(H_2O)_2]\cdot 5H_2O$ (**4**).

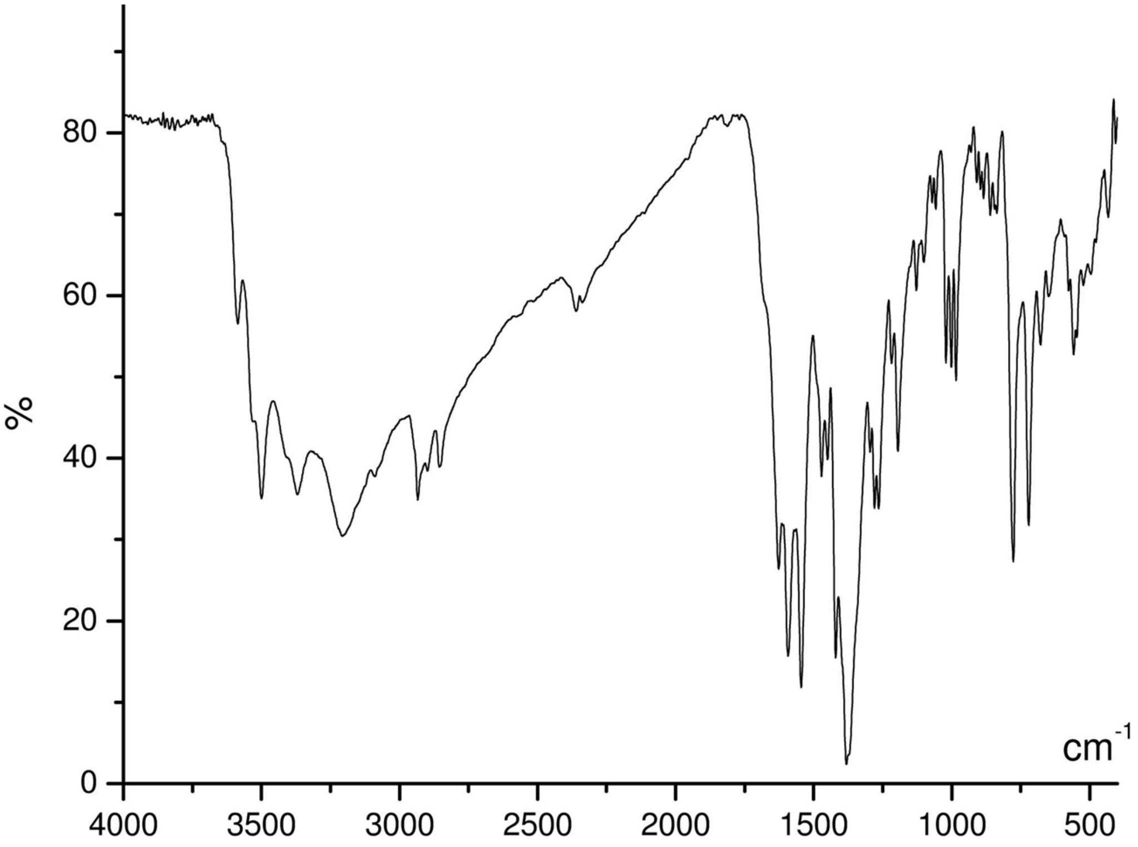

Figure S6. IR spectrum (KBr disk) of $[Cu_5(\mu\text{-}OH)_2\{HO\text{-}BDC\}_4(L)_2(H_2O)_2]\cdot6H_2O$ (**5**)

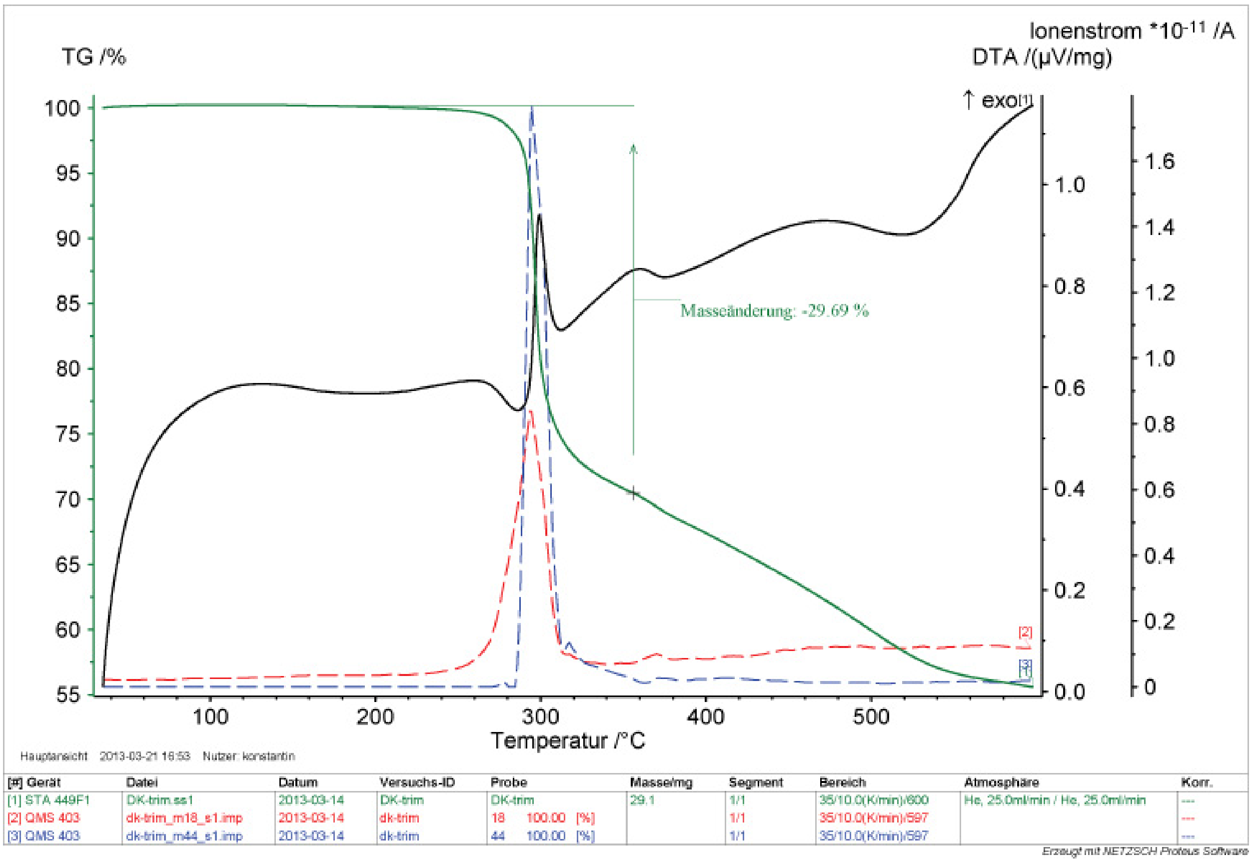

[#] Gerät	Datei	Datum	Versuchs-ID	Probe	Masse/mg	Segment	Bereich	Atmosphäre	Korr.
[1] STA 449F1	DK-trim.ss1	2013-03-14	DK-trim	DK-trim	29.1	1/1	35/10.0(K/min)/600	He, 25.0ml/min / He, 25.0ml/min	---
[2] QMS 403	dk-trim_m18_s1.imp	2013-03-14	dk-trim	18 100.00 [%]		1/1	35/10.0(K/min)/597		---
[3] QMS 403	dk-trim_m44_s1.imp	2013-03-14	dk-trim	44 100.00 [%]		1/1	35/10.0(K/min)/597		---

Figure S7. Thermoanalytical (TGA/DTA) curves for $[Cu_2(\mu\text{-}OH)\{TMA\}(L)(H_2O)]$ (**1**).

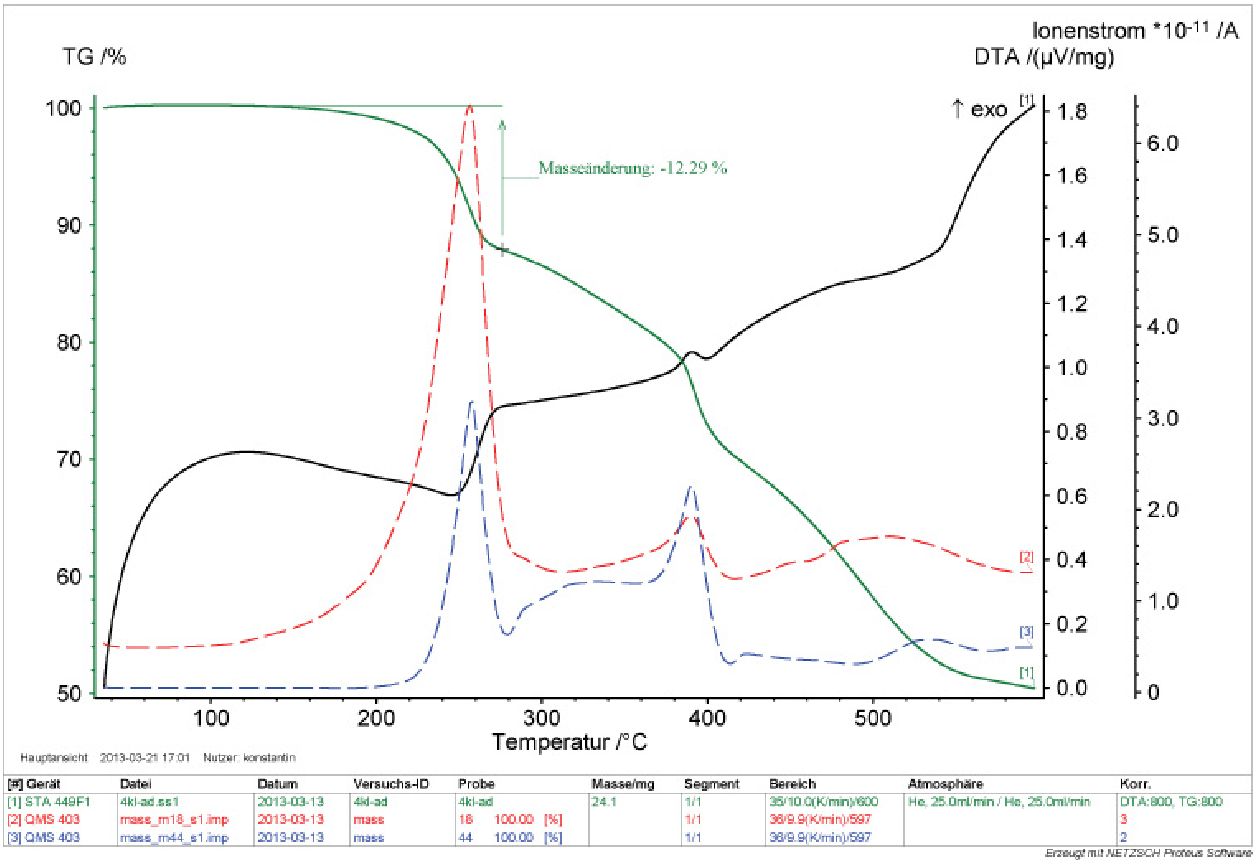

Hauptansicht 2013-03-21 17:01 Nutzer: konstantin

[#] Gerät	Datei	Datum	Versuchs-ID	Probe	Masse/mg	Segment	Bereich	Atmosphäre	Korr.
[1] STA 449F1	4kl-ad.ss1	2013-03-13	4kl-ad	4kl-ad	24.1	1/1	35/10.0(K/min)/600	He, 25.0ml/min / He, 25.0ml/min	DTA:800, TG:800
[2] QMS 403	mass_m18_s1.imp	2013-03-13	mass	18 100.00 [%]		1/1	36/9.9(K/min)/597		3
[3] QMS 403	mass_m44_s1.imp	2013-03-13	mass	44 100.00 [%]		1/1	36/9.9(K/min)/597		2

Erzeugt mit NETZSCH Proteus Software

Figure S8. Thermoanalytical (TGA/DTA) curves for $[Cu_4(\mu_3\text{-}OH)_2\{ATC\}_2(L)_2(H_2O)_2]\cdot H_2O$ (**2**)

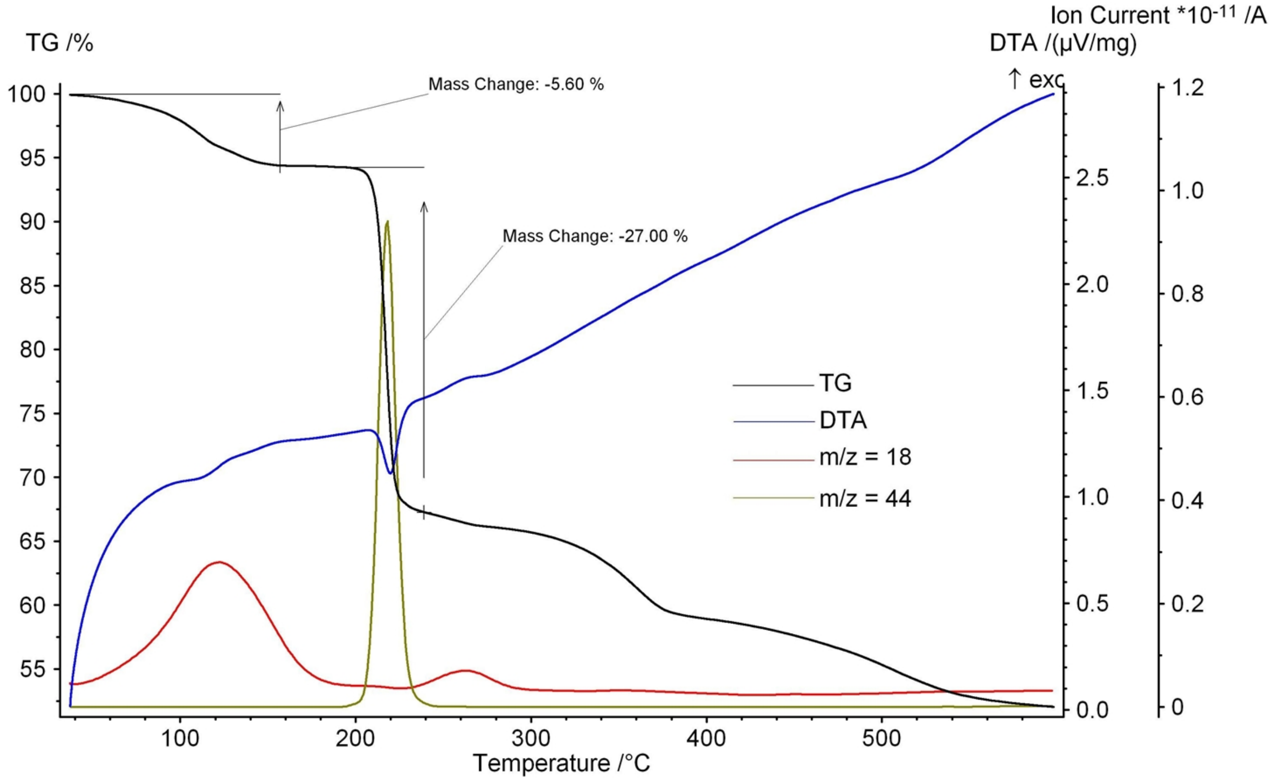

Figure S9. Thermoanalytical (TGA/DTA) curves for $[Cu_4(\mu_3\text{-}OH)_2\{TDC\}_3(L)_2(H_2O)_2]\cdot 7H_2O$ (**3**).

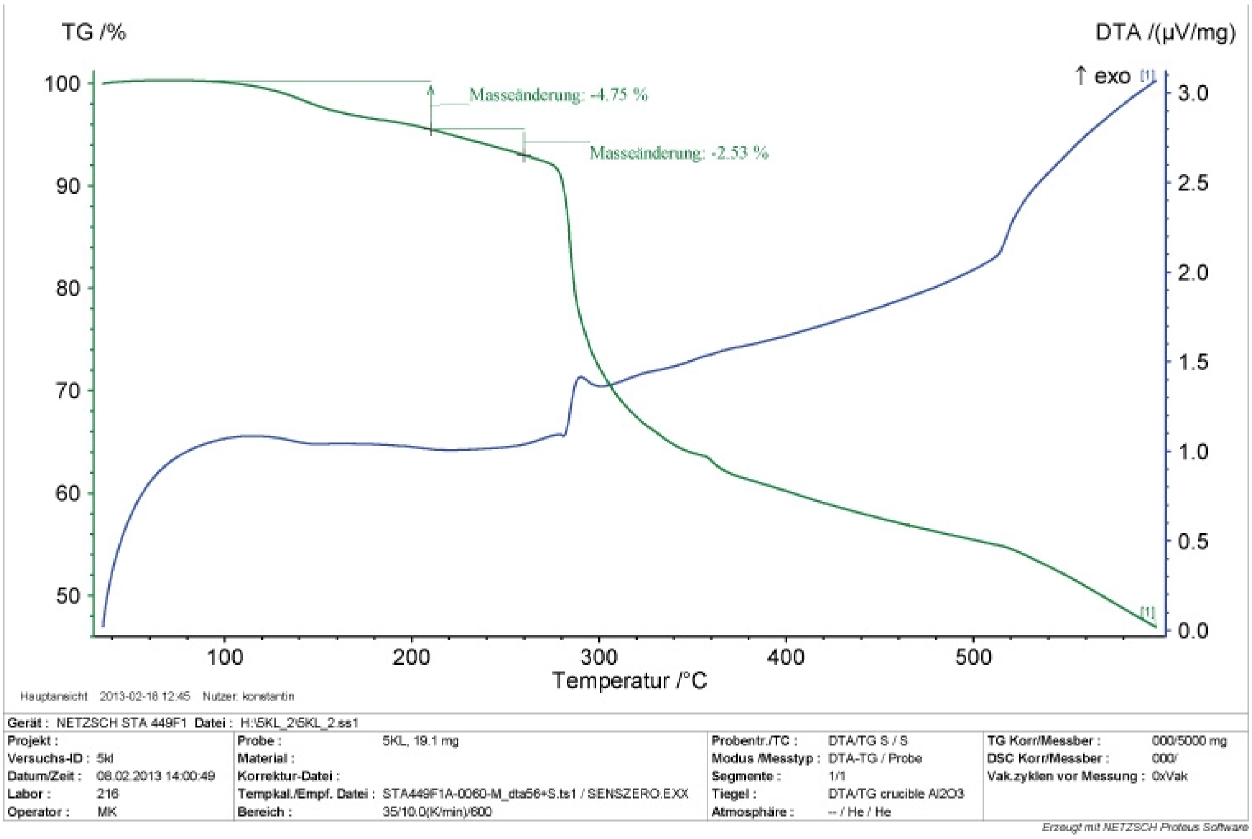

Hauptansicht 2013-02-18 12:45 Nutzer: konstantin

Gerät : NETZSCH STA 449F1 Datei : H:\5KL_2\5KL_2.ss1

Projekt :		Probe :	5KL, 19.1 mg	Probentr./TC :	DTA/TG S / S	TG Korr/Messber :	000/5000 mg
Versuchs-ID :	5kl	Material :		Modus /Messtyp :	DTA-TG / Probe	DSC Korr/Messber :	000/
Datum/Zeit :	08.02.2013 14:00:49	Korrektur-Datei :		Segmente :	1/1	Vak.zyklen vor Messung :	0xVak
Labor :	216	Tempkal./Empf. Datei :	STA449F1A-0060-M_dta56+S.ts1 / SENSZERO.EXX	Tiegel :	DTA/TG crucible Al2O3		
Operator :	MK	Bereich :	35/10.0(K/min)/600	Atmosphäre :	-- / He / He		

Erzeugt mit NETZSCH Proteus Software

Figure S10. Thermoanalytical (TGA/DTA) curves for *$[Cu_5(\mu\text{-}OH)_2\{BDC\}_4(L)_2(H_2O)_2]\cdot 5H_2O$* (**4**).

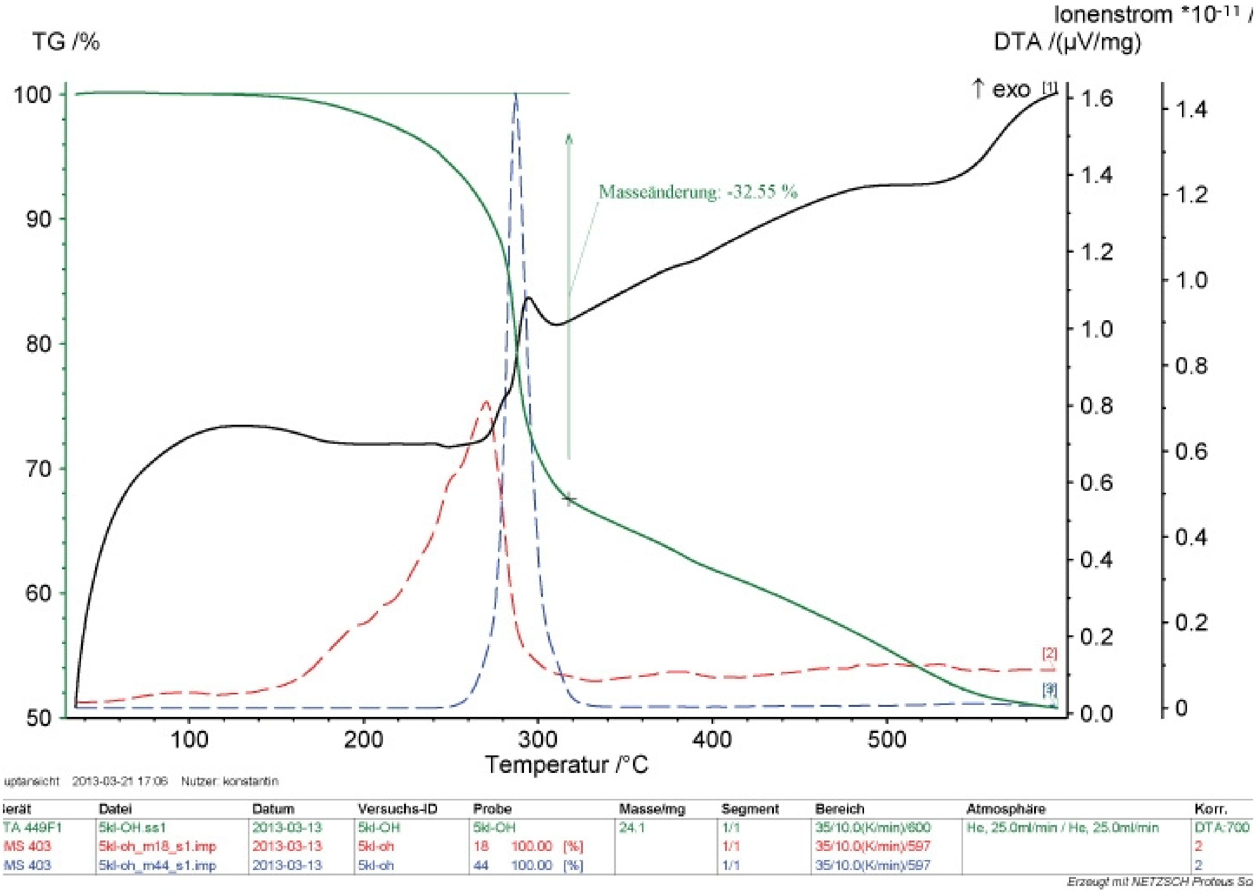

uptansicht 2013-03-21 17:06 Nutzer: konstantin

lerät	Datei	Datum	Versuchs-ID	Probe	Masse/mg	Segment	Bereich	Atmosphäre	Korr.
TA 449F1	5kl-OH.ss1	2013-03-13	5kl-OH	5kl-OH	24.1	1/1	35/10.0(K/min)/600	He, 25.0ml/min / He, 25.0ml/min	DTA:700
MS 403	5kl-oh_m18_s1.imp	2013-03-13	5kl-oh	18 100.00 [%]		1/1	35/10.0(K/min)/597		2
MS 403	5kl-oh_m44_s1.imp	2013-03-13	5kl-oh	44 100.00 [%]		1/1	35/10.0(K/min)/597		2

Erzeugt mit NETZSCH Proteus So

Figure S11. Thermoanalytical (TGA/DTA) curves for *$[Cu_5(\mu\text{-}OH)_2\{HO\text{-}BDC\}_4(L)_2(H_2O)_2]\cdot 6H_2O$* (**5**)

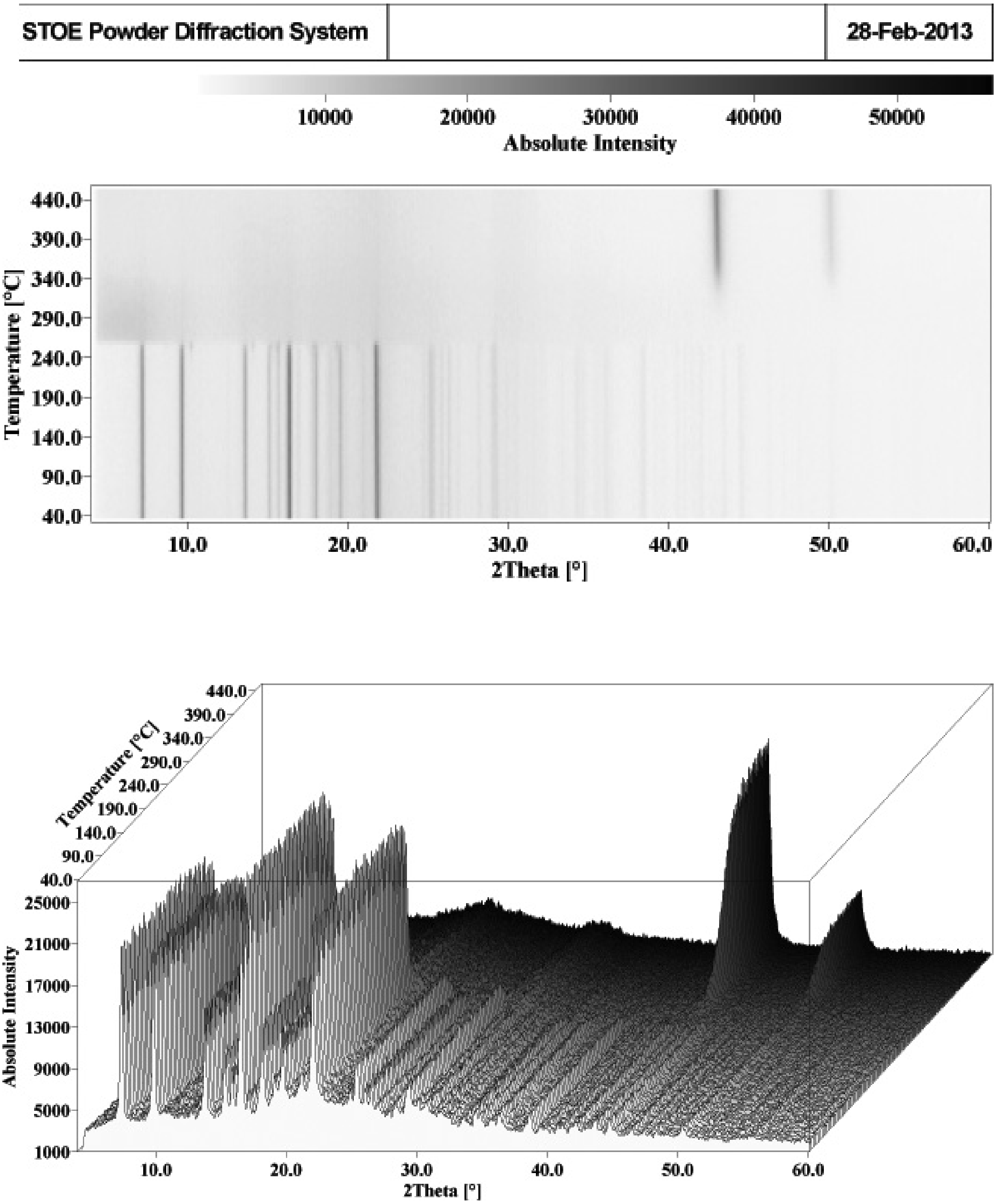

Figure S12. Thermo-XRPD patterns (2D and 3D visualization) for *[Cu$_2$(μ-OH){TMA}(L)(H$_2$O)]* (**1**).

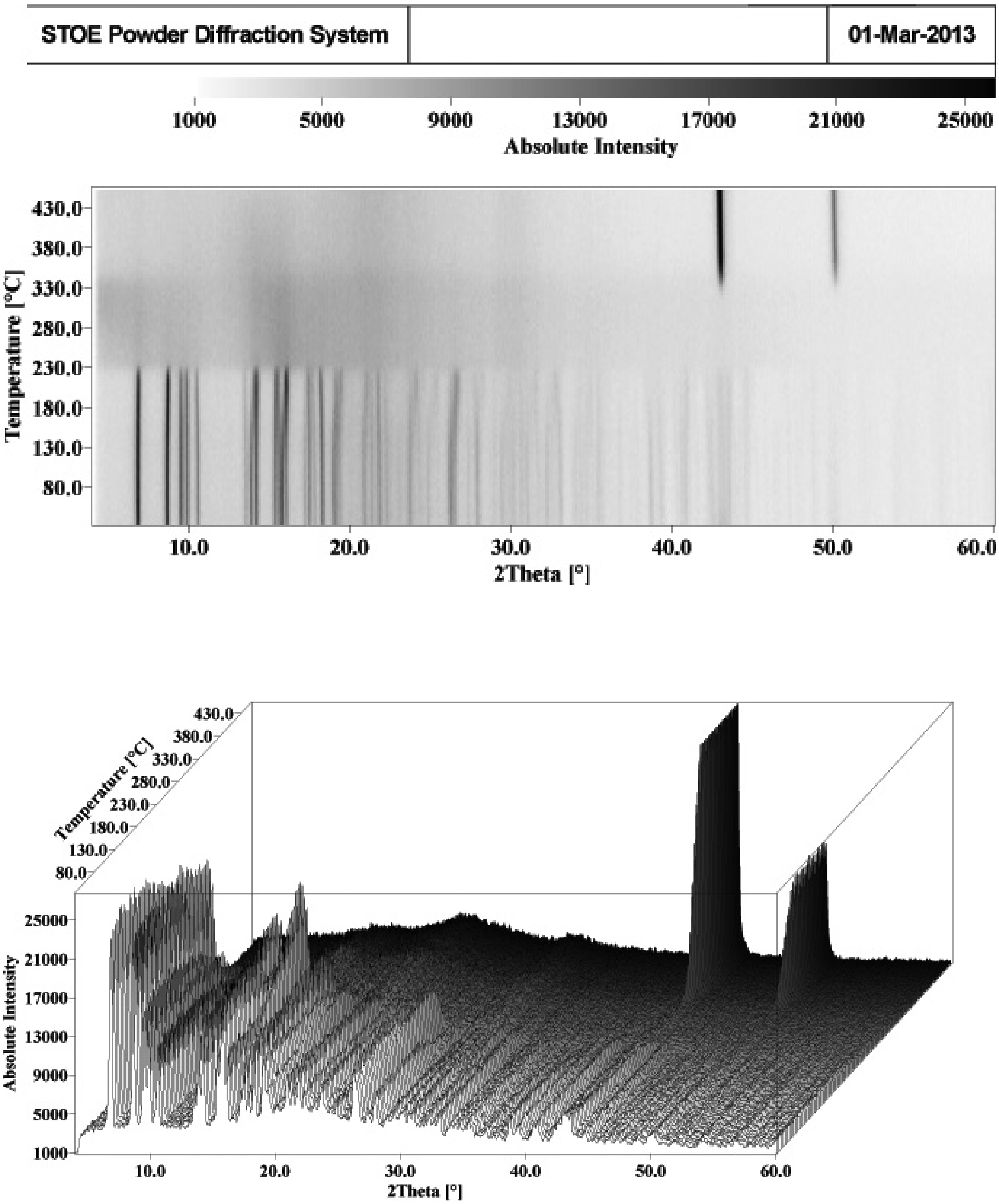

Figure S13. Thermo-XRPD patterns (2D and 3D visualization) for $[Cu_4(\mu_3\text{-}OH)_2\{ATC\}_2(L)_2(H_2O)_2]\cdot H_2O$ (**2**)

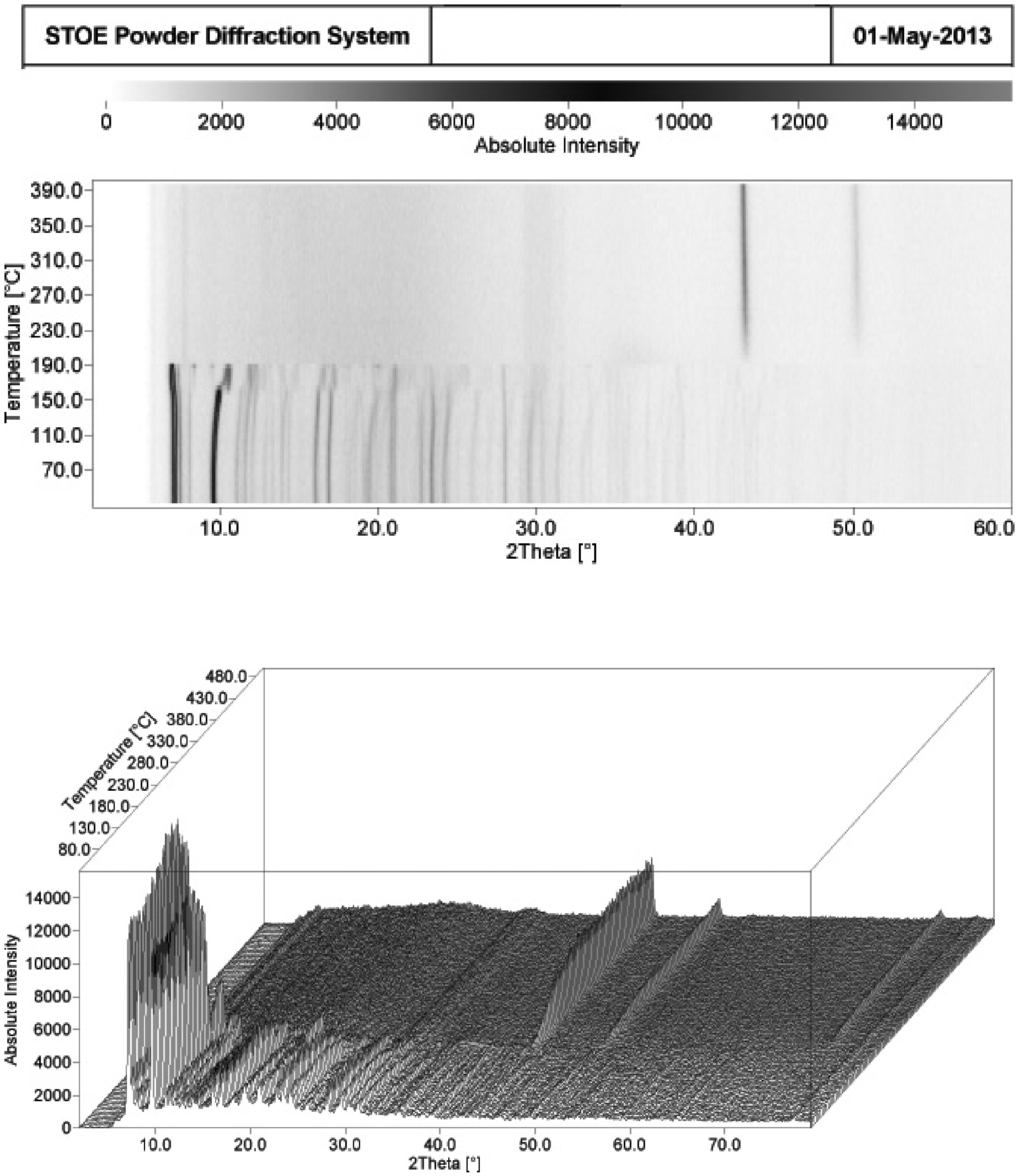

Figure S14. Thermo-XRPD patterns (2D and 3D visualization) for $[Cu_4(\mu_3\text{-}OH)_2\{TDC\}_3(L)_2(H_2O)_2]\cdot 7H_2O$ (**3**).

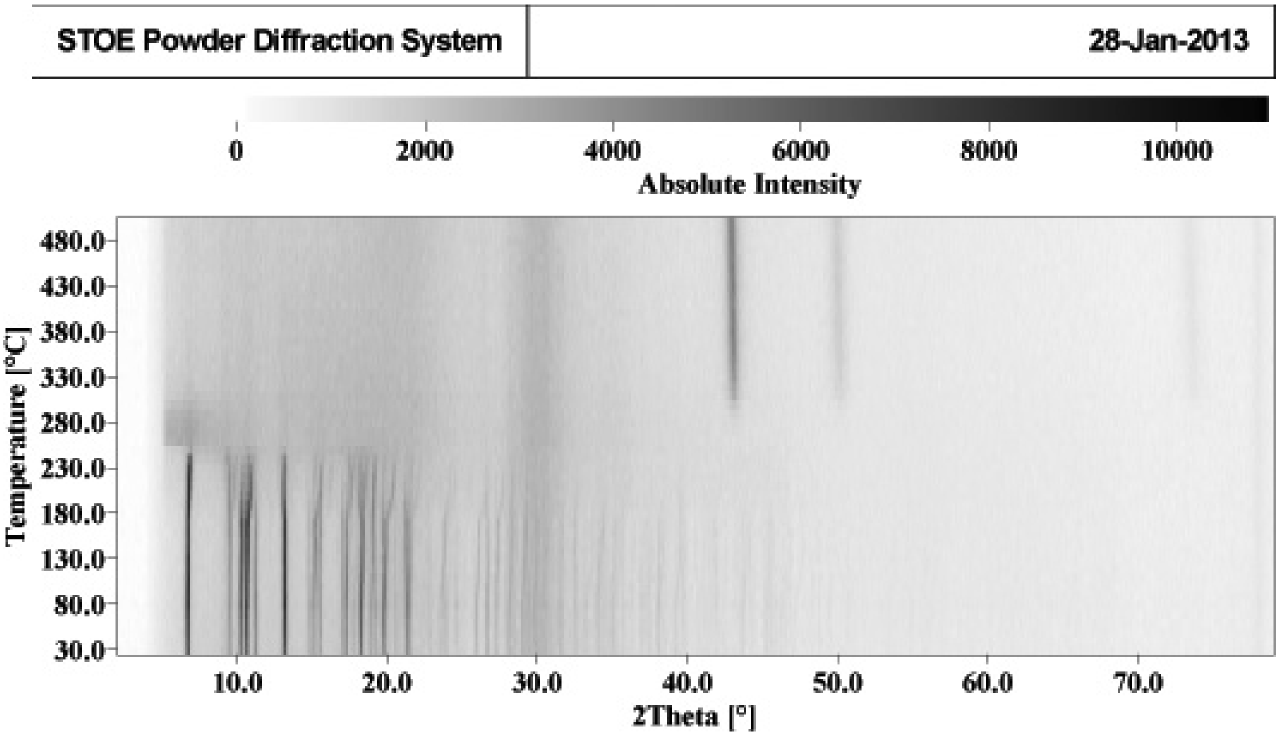

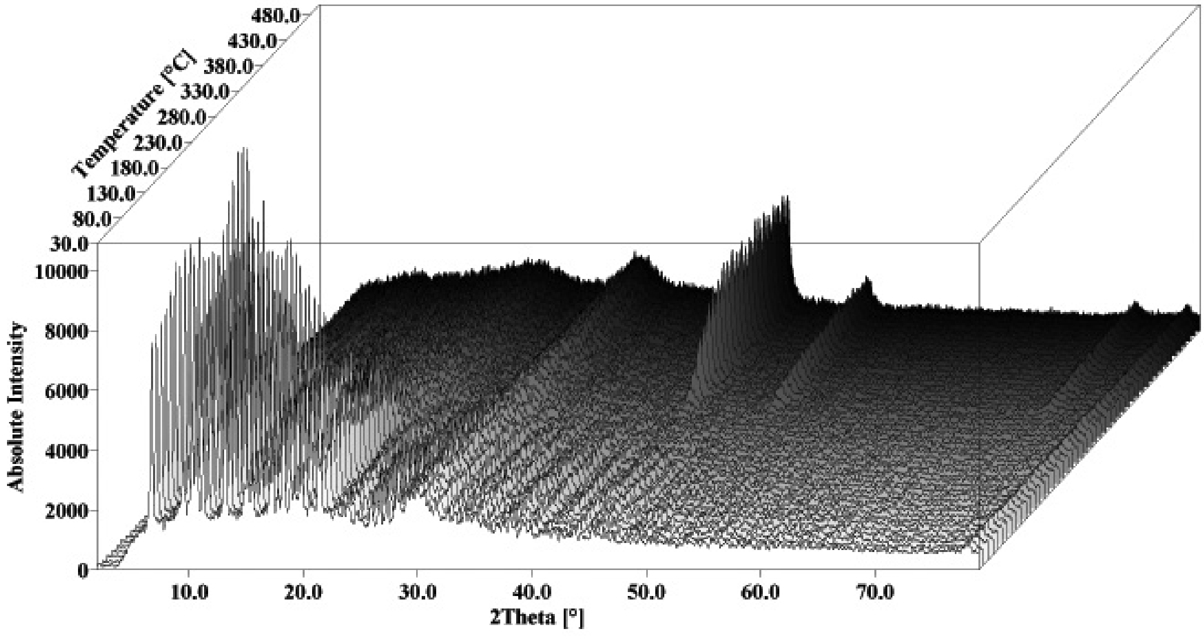

Figure S15. Thermo-XRPD patterns (2D and 3D visualization) for $[Cu_5(\mu\text{-}OH)_2\{BDC\}_4(L)_2(H_2O)_2]\cdot 5H_2O$ (**4**).

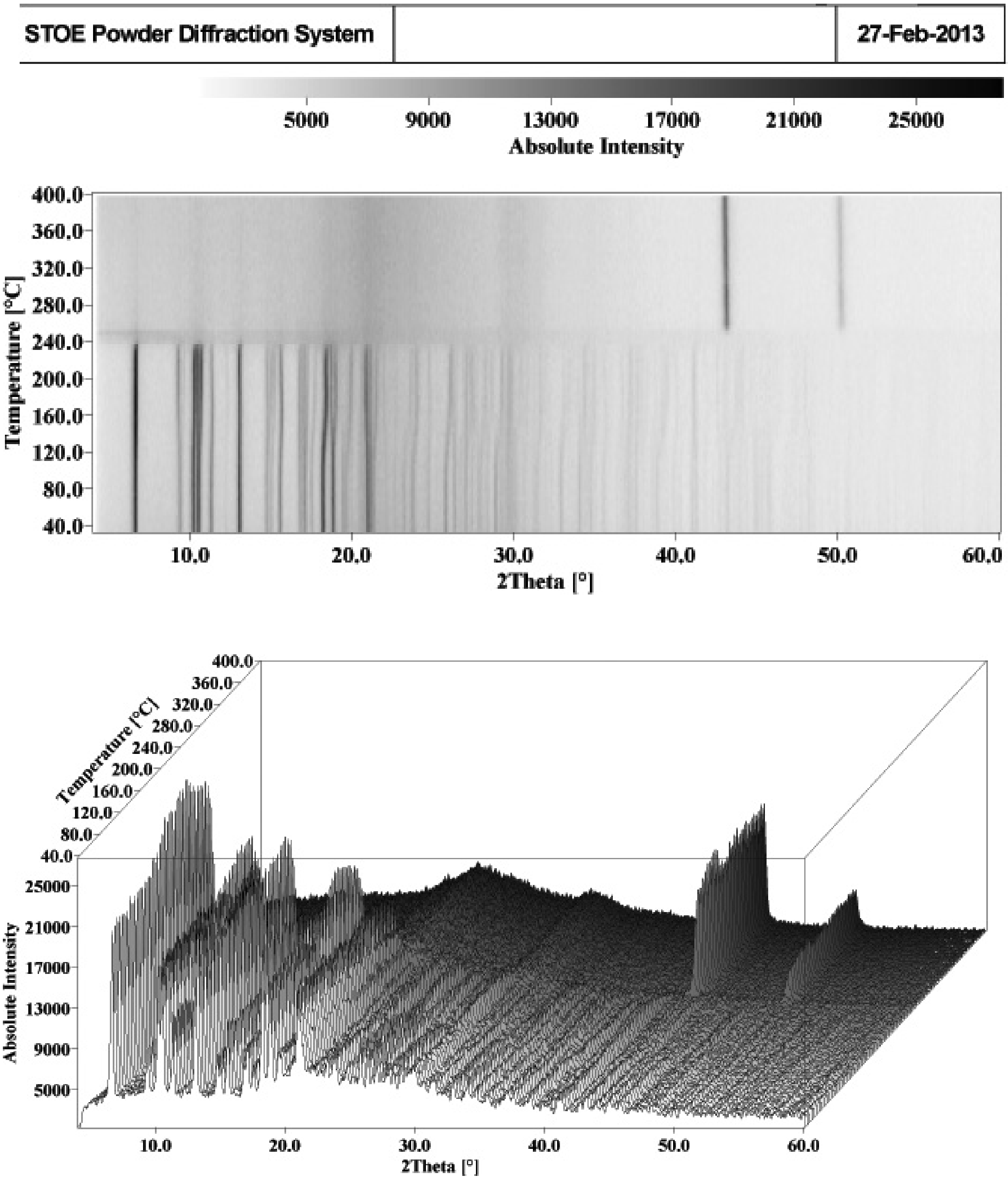

Figure S16. Thermo-XRPD patterns (2D and 3D visualization) for $[Cu_5(\mu\text{-}OH)_2\{HO\text{-}BDC\}_4(L)_2(H_2O)_2]\cdot 6H_2O$ (**5**)

5. Features of the crystal structure refinements

The diffraction data were collected with graphite-monochromated Mo Kα radiation (λ = 0.71073 Å). Measurements for **1** at 213K and for **4** (**4a**: 296K, **4b**: 105K) were made using a Stoe Imaging Plate Diffraction System, φ oscillation scans (φ 0→180°; Δφ = 0.9°; exposure times 8-10 min pre frame) (numerical absorption correction using X-RED and X-SHAPE).[1] Measurements for **2**, **3** and **5** were performed at 173 K on a Bruker APEXII CCD area-detector diffractometer (ω scans). The data were corrected for Lorentz-polarization effects and for the effects of absorption (multi-scans method). The structures were solved by direct methods and refined by full-matrix least-squares on F^2 using the SHELX-97 package.[2] Commonly, the CH-hydrogen atoms were added geometrically, with $U_{iso} = 1.2U_{eq}$(C) and OH-hydrogen atoms were located and included with fixed d(O-H) = 0.85 Å and $U_{iso} = 1.5U_{eq}$(O).

[1] (a) Stoe & Cie. X-SHAPE. Revision 1.06, Stoe & Cie GmbH, Darmstadt, Germany, **1999**; (b) Stoe & Cie. X-RED. Version 1.22, Stoe & Cie GmbH, Darmstadt, Germany, **2001**.

[2] (a) Sheldrick, G. M. *Acta Crystallogr.* **1990**, *A46*, 467; (b) Sheldrick, G. M. *Acta Crystallogr.* **2008**, *A64*, 112.

5.1. [Cu_2(μ-OH){TMA}(L)(H_2O)] (1).

Main feature of the crystal structure refinement was associated with disorder within the binuclear cluster. It is equally disordered over two positions (one Cu ion, μ-OH and aqua ligand; one of the pyridazine cycles is also disordered by rotation along N1---C2 axis, adopting two orientations, See Figures **S17** and **S18**). Attempted solution and refinements in space groups of lower symmetry (either monoclinic *C*, monoclinic *P* or triclinic lattices were considered) did not afford an ordered model. Both contributions of the disorder (PART -1 and PART -2) were freely refined anisotropically, without any restraints or constraints in the geometry and thermal motion, and the hydrogen atoms of these fragments were added as stated above with partial occupancy factors of 0.5.

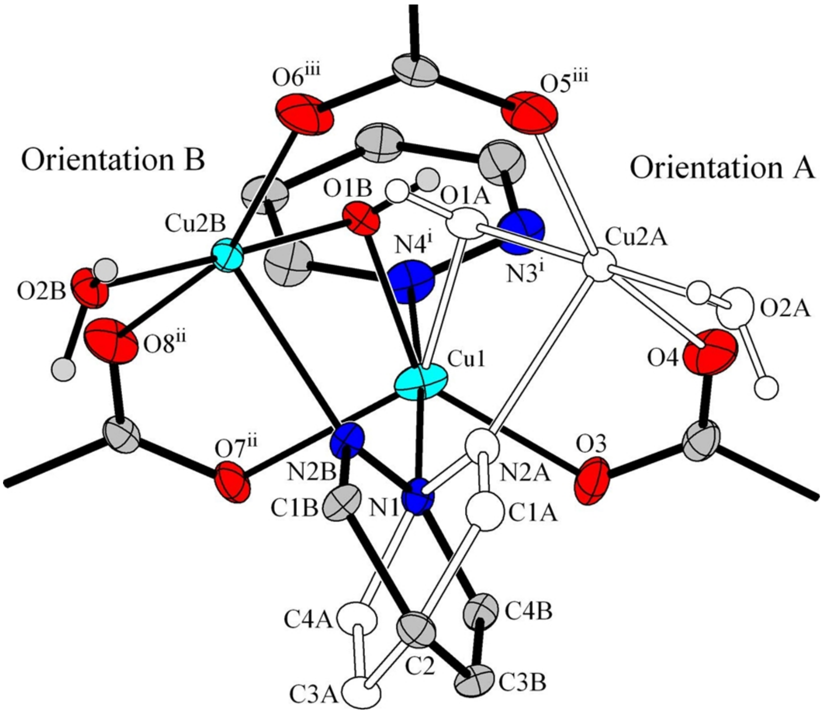

Figure S17. Refined disordering scheme for the binuclear cluster fragment in the structure of **1**, showing also disorder of the pyridazine cycle, as rotation along N1---C2 axis, with N1 and C2 atoms being common for two components of the disorder. Thermal ellipsoids are at 35% probablility level and two components of the disorder are indicated with bold and open bonds. Note anisotropy of thermal motion for the Cu1 atom.

Table S1. Hydrogen-bond geometry (Å, °) for structure of **1**.

Donor (D)	Hydrogen (H)	Acceptor (A)[a]	D-H	H···A	D···A	∠DH···A
O2A	H1WA	$O5^{iv}$	0.85	1.80	2.648(4)	174
O2A	H2WA	$O4^{v}$	0.85	1.93	2.737(4)	158
O2B	H1WB	$O8^{vi}$	0.85	1.86	2.694(4)	165
O2B	H2WB	$O6^{v}$	0.85	1.84	2.655(4)	160
O1A	H1OA	$O6^{iii}$	0.85	2.27	3.013(5)	146
O1B	H1OB	$O5^{iii}$	0.85	2.39	3.131(4)	146

[a] Symmetry codes: (iii) *x*, 1-*y*, 0.5+*z*; (iv) 1-*x*, *y*, 0.5-*z*; (v) 1-*x*, 1-*y*, 1-*z*; (vi) 1-*x*, -*y*, 1-*z*.

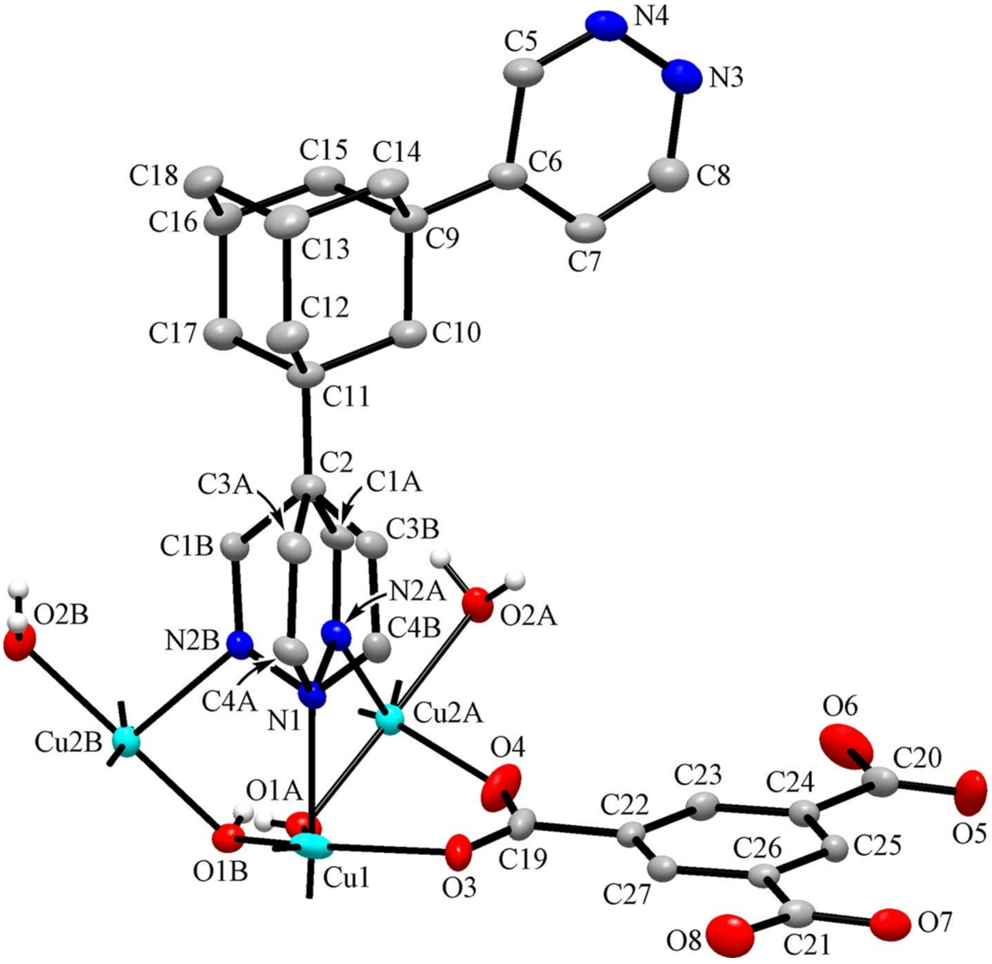

Figure S18. Unique portion of the structure **1**, showing the atom labeling scheme. Thermal ellipsoids are at 40% probablility level and CH-hydrogen atoms are omitted for clarity. Atoms of the disordered fragment (marked with A and B indices) were refined with 0.5 partial occupancy factors.

5.2. $[Cu_4(\mu_3\text{-}OH)_2\{ATC\}_2(L)_2(H_2O)_2]\cdot H_2O$ (2)

The refinement was essentially standard and the hydrogen atoms were considered as stated above. The solvate water molecule (O3W) is equally disordered over two closely separated positions related by inversion [O3W··· O3W (1-x, 1-y, 1-z) = 1.36 Å]. The O3W atom was refined with 0.5 occupancy factor and it was left isotropic due to the relatively high value of U_{iso} = 0.244(9) Å^2. The hydrogen atoms were not added to this disordered water molecule.

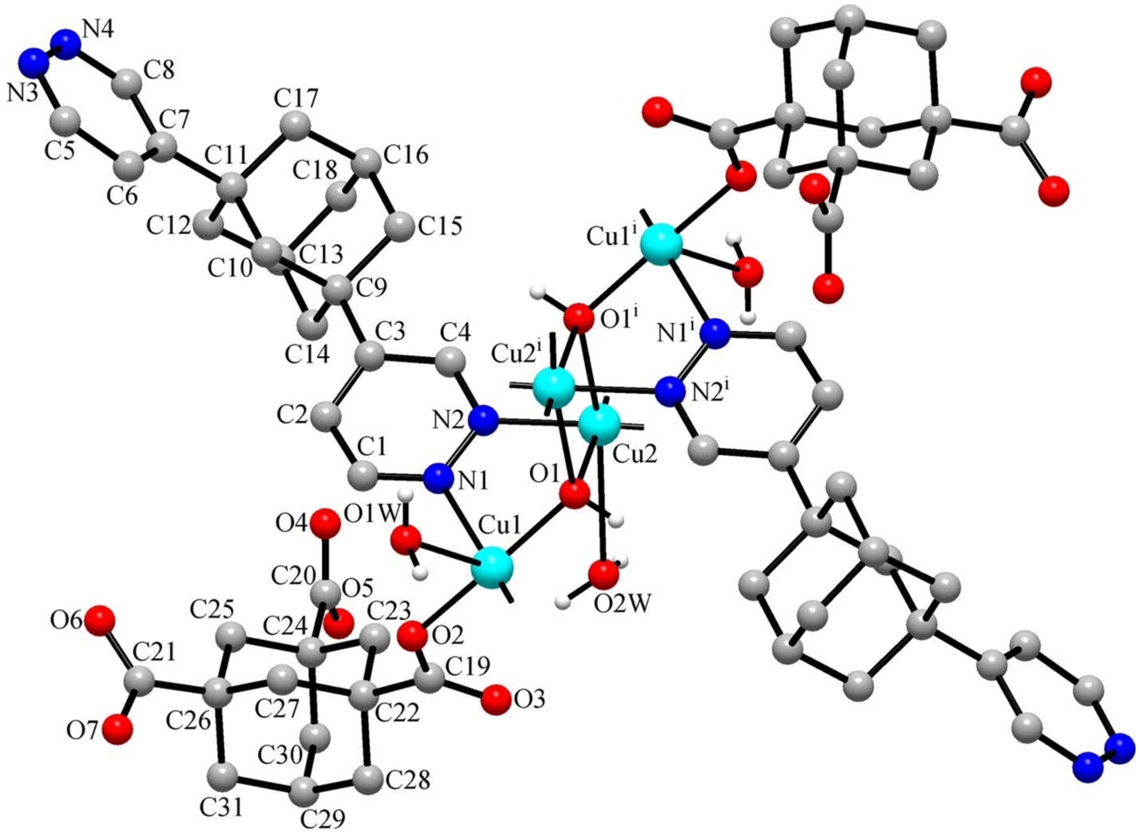

Figure S19. Fragment of the structure **2**, showing the atom labeling scheme (CH-hydrogens and disordered solvate water molecule are omitted for clarity). Symmetry code: (i) –*x*, 2-*y*, 1-*z*.

Table S2. Hydrogen-bond geometry (Å, °) for structure of **2**.

Donor (D)	Hydrogen (H)	Acceptor (A)[a)]	D-H	H···A	D···A	∠DH···A
O1	H1O	O7^{ii}	0.85	2.00	2.796(4)	157
O1W	H1W	N3^{iv}	0.85	2.31	2.942(5)	131
O1W	H2W	O6^{v}	0.85	2.07	2.791(4)	142
O2W	H3W	O3	0.85	2.06	2.838(5)	152
O2W	H4W	O4^{iii}	0.85	2.08	2.760(5)	136
O3W[b)]	-	O4	-	-	2.93(2)	-
O3W	-	O4^{iii}	-	-	2.91(2)	-

[a)] Symmetry codes: (ii) -1+*x*, *y*, *z*; (iii) 1-*x*, 1-*y*, 1-*z*; (iv) *x*, *y*, -1+*z*; (v) 1-*x*, 2-*y*, 1-*z*. [b)] H-atoms were not added to the disordered water molecule O3W.

5.3. $[Cu_4(\mu_3\text{-}OH)_2\{TDC\}_3(L)_2(H_2O)_2]\cdot 7H_2O$ (**3**).

One of the present thiophenedicarboxylate ligands is equally disordered over center of inversion, giving two overlapping orientations. The disorder was resolved without any restraints in geometry and all atoms were refined anisotropically, with similarity restraints (SIMU) for the thermal motion of carbon atoms and rigid bond restrains for the thermal motion of carboxylic groups (DELU). The H-atoms were added to the disordered fragment with partial occupancy factors of 0.5. Further, the disorder of bulky organic ligand effects partial disordering in the region of neighboring solvate water molecules. Two water molecules (O3W and O4W) are situated closely to this TDC^{2-} fragment and have corresponding partial occupancies of 0.5, depending on orientation of the disordered TDC^{2-}. These oxygen atoms were refined anisotropically, but H-atoms were not added. Another water molecule is similarly disordered nearly TDC^{2-}, but its 0.5 partially occupied position is also splitted between two closely separated positions (O51W to O52W 1.40 Å). In this case the refined partial contributions were 0.30 and 0.20, these atoms O51W and O52W were refined isotropically and H-atoms were not added. Two other solvate water molecules (O1W and O2W) are ordered, their refinement was standard, in the anisotropic approximation, OH-hydrogen atoms were located and included with fixed d(O-H) = 0.85 Å and $U_{iso} = 1.5U_{eq}$(O).

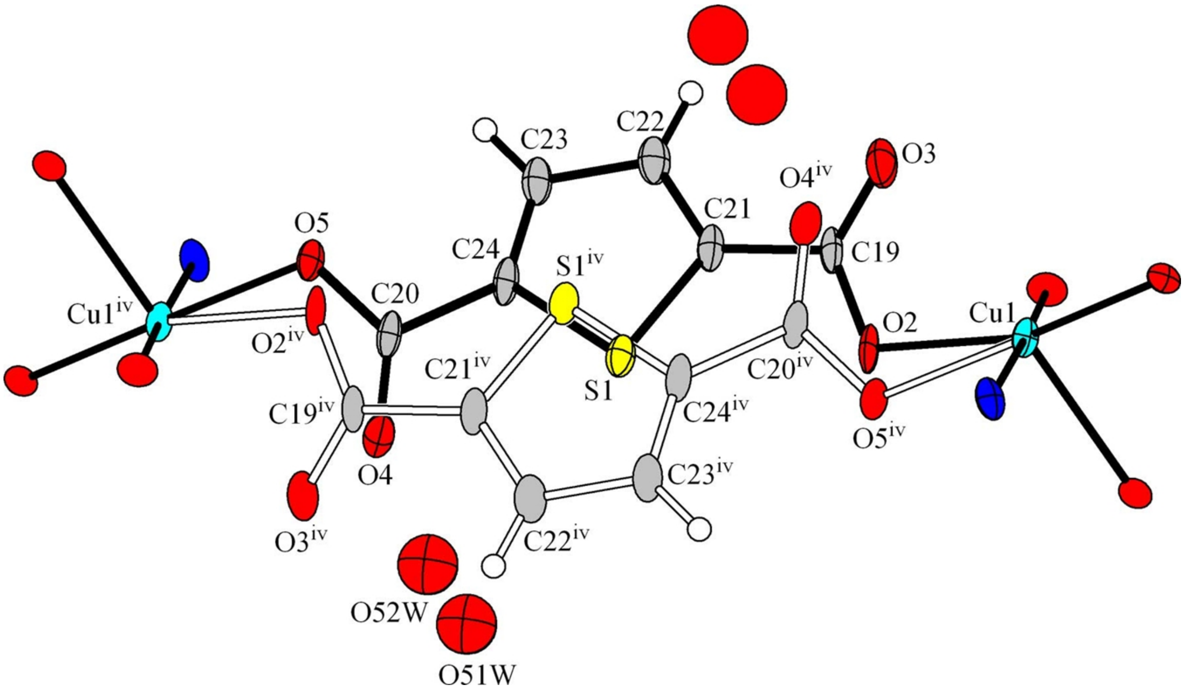

Figure S20. Refined disordering scheme for one of the bridging 2,5-thiophenedicarboxylate ligands in structure of **3**. Thermal ellipsoids are at 40% probability level. Two components of the disorder (marked with bold and open bonds) are related by inversion (symmetry code (iv) $-x$, $2-y$, $-z$).

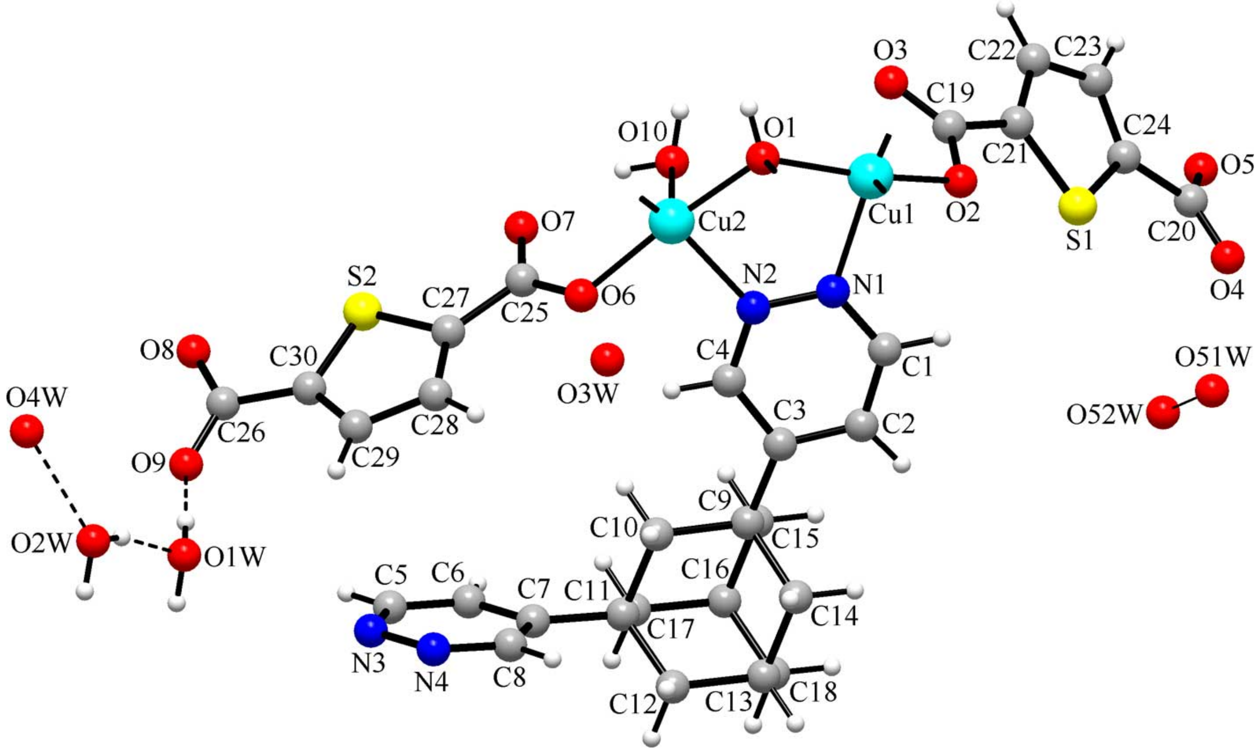

Figure S21. Unique portion of the structure **3**, showing the atom labeling scheme (Water molecules O3W, O4W, O51W and O52W, and thiphenedicarboxylate ligand referenced by the sulfur atom S1 are disordered, See Figure **S20**).

Table S3. Hydrogen-bond geometry (Å, º) for structure of **3**.

Donor (D)	Hydrogen (H)	Acceptor (A)a)	D-H	H···A	D···A	∠DH···A
O1	H1H	O9^{ii}	0.85	2.19	2.878(3)	138
O10	H1W	O7	0.85	1.92	2.691(4)	150
O10	H2W	O1W^{iii}	0.85	1.93	2.780(4)	174
O1W	H3W	O9	0.85	1.90	2.747(4)	171
O1W	H4W	O9^{v}	0.85	1.98	2.825(4)	171
O2W	H5W	O3^{vi}	0.85	2.06	2.794(8)	144
O2W	H6W	O1W	0.85	1.92	2.754(5)	167

a) Symmetry codes: (ii) -0.5+*x*, 2.5-*y*, -0.5+*z*; (iii) 1.5-*x*, 0.5+*y*, 0.5-*z*; (v) 2–*x*, 2-*y*, 1-*z*; (vi) 1.5-*x*, -0.5+*y*, 0.5-*z*.

5.4. $[Cu_5(\mu\text{-}OH)_2\{BDC\}_4(L)_2(H_2O)_2]\cdot 5H_2O$ (4).

The refinement of the framework portion (including coordinated water molecules) was standard. The CH-hydrogen atoms were added geometrically, with $U_{iso} = 1.2U_{eq}$(C) and OH-hydrogen atoms were located and included with fixed d(O-H) = 0.85 Å and $U_{iso} = 1.5U_{eq}$(O). The solvate water molecules, however, are disordered. Two of them adopt pairs of closely separated positions (O11W and O12W at 0.89 Å; O21W and O22W at 0.72 Å) and the third one (occupancy 0.50) is at 1.97 Å near O11W position. The refined partial occupancy factors were

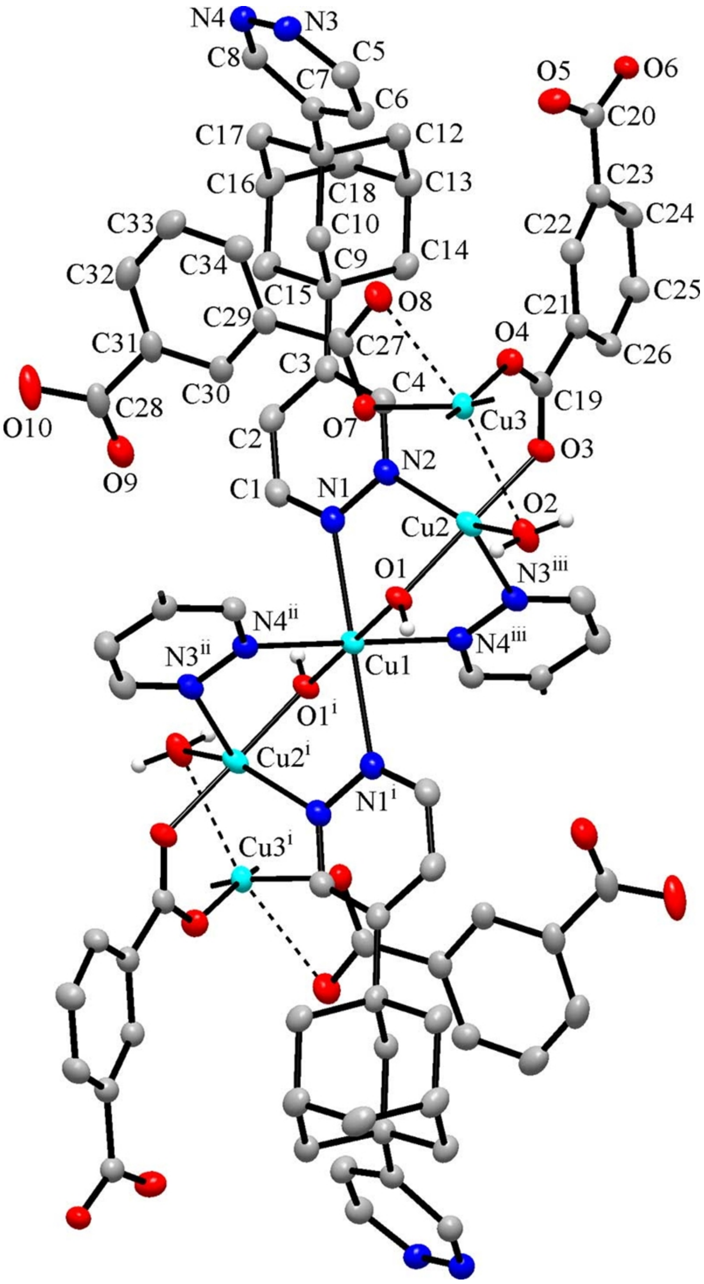

Figure S22. View of pentanuclear cluster in 4, showing the atom labeling scheme. Thermal ellipsoids are at 40% probablility level and CH-hydrogen atoms are omitted for clarity.

Table S4. Hydrogen-bond geometry (Å, °) for structure of **4**.

At 296K (**4a**)

Donor (D)	Hydrogen (H)	Acceptor (A)[a]	D-H	H···A	D···A	∠DH···A
O1	H1H	O21W$^{\mathrm{iv}}$ [b]	0.85	2.15	3.003(14)	173
O1	H1H	O22W$^{\mathrm{iv}}$ [b]	0.85	1.96	2.783(7)	161
O2	H1W	O5$^{\mathrm{iv}}$	0.85	1.84	2.648(3)	158
O2	H2W	O9$^{\mathrm{v}}$	0.85	1.90	2.707(3)	157
O22W [b]	-	O5	-	-	2.743(8)	-
O22W [b]	-	O12W [b]	-	-	2.795(16)	-
O21W [b]	-	O5	-	-	2.830(14)	-
O21W [b]	-	O11W [b]	-	-	2.75(2)	-
O12W [b]	-	O8	-	-	2.721(14)	-
O12W [b]	-	O3W [b]	-	-	2.924(13)	-

At 105K (**4b**)

Donor (D)	Hydrogen (H)	Acceptor (A)[a]	D-H	H···A	D···A	∠DH···A
O1	H1H	O21W$^{\mathrm{iv}}$ [b]	0.85	2.18	3.021(7)	172
O1	H1H	O22W$^{\mathrm{iv}}$ [b]	0.85	1.92	2.744(4)	164
O2	H1W	O5$^{\mathrm{iv}}$	0.85	1.84	2.640(2)	156
O2	H2W	O9$^{\mathrm{v}}$	0.85	1.91	2.715(2)	156
O22W [b]	-	O5	-	-	2.751(4)	-
O22W [b]	-	O12W [b]	-	-	2.763(5)	-
O21W [b]	-	O5	-	-	2.860(7)	-
O21W [b]	-	O11W [b]	-	-	2.836(9)	-
O12W [b]	-	O8	-	-	2.749(4)	-
O12W [b]	-	O3W [b]	-	-	2.850(6)	-

[a] Symmetry codes: (iv) 1.5–x, 0.5+y, 0.5-z; (v) 1+x, y, z.

[b] Partially occupied positions.

0.6 and 0.4 in the first two cases. These disordered oxygen atoms (2.5 in assymmetric part, or 5 equivalents per centrosymmetric pentanuclear unit) were refined anisotropically giving reasonable thermal parameters (U_{eq} = 0.0329(8)-0.0476(16) Å^2), but the hydrogen atoms were not added due to the disorder.

5.5. $[Cu_5(\mu\text{-}OH)_2\{HO\text{-}BDC\}_4(L)_2(H_2O)_2]\cdot 6H_2O$ (**5**)

The refinement was standard and no disordered moieties were found in the structure. The CH-hydrogen atoms were added geometrically, with $U_{iso} = 1.2U_{eq}(C)$ and OH-hydrogen atoms were located and included with fixed d(O-H) = 0.85 Å and $U_{iso} = 1.5U_{eq}(O)$.

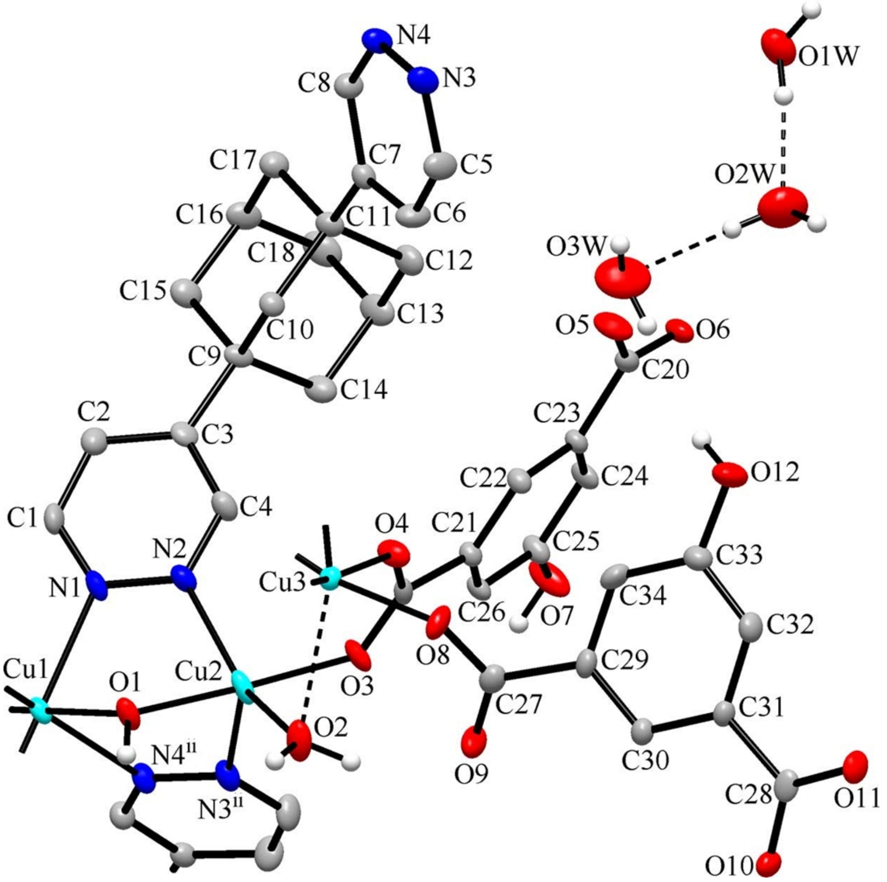

Figure S23. Unique portion of the structure of **5**, showing the atom labeling scheme (half of the pentanuclear cluster; Cu1 ion is situated on the center of inversion). Thermal ellipsoids are at 40% probablility level and CH-hydrogen atoms are omitted for clarity.

Table S5. Hydrogen-bond geometry (Å, °) for structure of **5**.

Donor (D)	Hydrogen (H)	Acceptor (A)[a)]	D-H	H···A	D···A	∠DH···A
O1	H1H	O1W^{vi}	0.85	2.14	2.935(3)	156
O2	H1W	O5^{iv}	0.85	1.93	2.660(3)	143
O2	H2W	O9	0.85	1.95	2.688(4)	144
O7	H1O	O11^{vii}	0.85	1.90	2.726(3)	162
O12	H2O	O1W^{iv}	0.85	1.87	2.722(4)	176
O1W	H3W	O5^{viii}	0.85	1.92	2.733(4)	159
O1W	H4W	O2W	0.85	1.83	2.676(4)	171
O2W	H5W	O3W	0.85	2.00	2.829(5)	165
O2W	H6W	O11^{ix}	0.85	2.00	2.794(4)	154
O3W	H7W	O7^{x}	0.85	2.32	3.109(5)	154
O3W	H8W	O8^{viii}	0.85	1.99	2.828(4)	169

[a)] Symmetry codes: (iv) $-x$, $-0.5+y$, $0.5-z$; (vi) x, $-1+y$, z; (vii) $1+x$, $0.5-y$, $0.5+z$; (viii) $-x$, $0.5+y$, $0.5-z$; (ix) $-1-x$, $0.5+y$, $0.5-z$; (x) $-x$, $1-y$, $1-z$.

Magnetic data

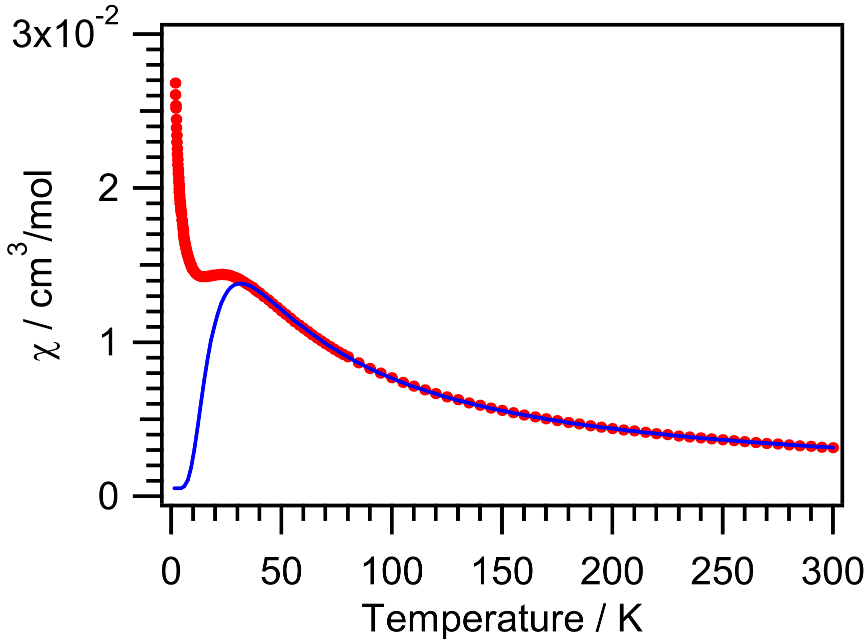

Figure S24. Thermal variation of χ_m for **2** (the solid line is drawn based on the Bleaney-Bowers equation).

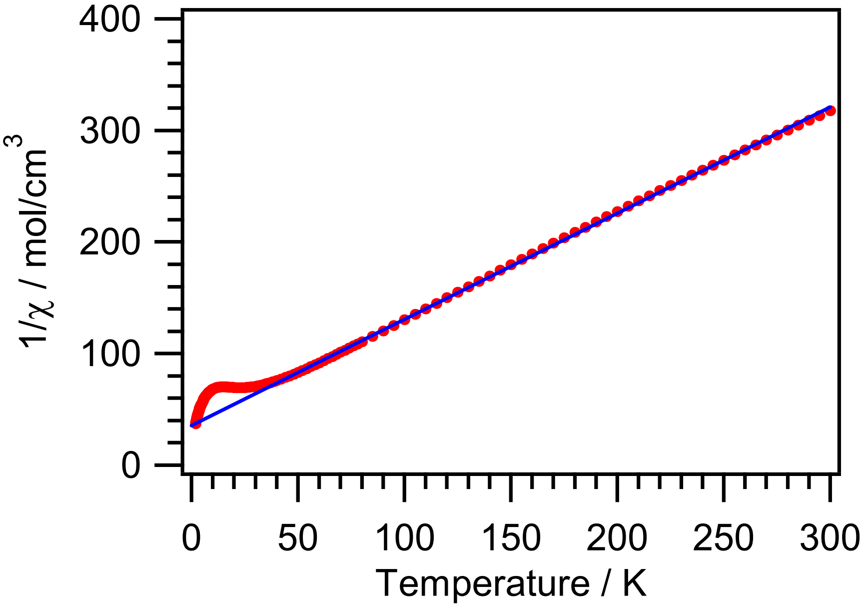

Figure S25. Inverse magnetic susceptibility versus temperature for **2** (the solid line represents a Curie-Weiss fit in the temperature range 50 – 300 K).